Article

Not peer-reviewed version

Primordial Axion Stars and Galaxy Halos Formation

Alexander I Nesterov *

Posted Date: 2 August 2024

doi: 10.20944/preprints202408.0033.v1

Keywords: Dark matter; Axions; Axion stars

Article

Primordial Axion Stars and Galaxy Halos Formation

Alexander Nesterov

University of Guadalajara; nesterov@academicos.udg.mx

Abstract: Primordial axion stars, hypothetical stars formed from axions, could play an essential role in forming galaxy halos. These stars could have originated in the early universe shortly after the Big Bang. We show that while "normal" axions coalesce into a gravitationally bound Bose-Einstein condensate, forming a dense object - an axion star, the ultralight axions could act as the initial seeds for galaxy halos.

Keywords: dark matter; axions; axion stars

Introduction

The axions are one of the favorite cold dark matter (CDM) candidates [1–3,26]. Initially, they were invented to solve the strong CP problem: Why does quantum chromodynamics (QCD) not break the CP-symmetry? The Peccei-Quinn (PQ) theory, solving this problem, leads to the existence of very light axions [4–7]. Since the axions have a tiny mass and extraordinarily weak coupling to matter and radiation, it would be challenging to detect them. Efforts toward detecting axions include a wide range of technologies [8–10].

The massless axion arises due to a spontaneous breaking of the $U(1)_{PQ}$ symmetry. The axion acquires a mass during the QCD phase-transition, following the PQ phase-transition. In terms of the axion decay constant, f_a, the axion mass induced by QCD instantons can be written as $m \approx 6\,\mu\text{eV}\left(10^{12}\,\text{GeV}/f_a\right)$ [11,12]. More precise estimation of the axion mass yields [13]

$$m_a \approx 5.7\mu\text{eV}\left(\frac{10^{12}\,\text{GeV}}{f_a}\right). \tag{1}$$

Cosmological and astrophysical constraints restrict the value of the decay constant and leave the allowed QCD axion mass window as $6\,\mu\text{eV} \leqslant m \leqslant 2000\,\mu\text{eV}$ [14]. Recent calculations of the axion mass, based on high-temperature lattice QCD, lead to the more narrow window: $50\,[\mu\text{eV}] \leqslant m \leqslant 1.5\cdot 10^3\,[\mu\text{eV}]$ [15]. The axions with the mass range $10^{-33}\text{eV} \lesssim \text{m} \lesssim 10^{-18}\text{eV}$ are known as ultralight axions (ULAs). The mass of ULA's can be estimated as follows [16,17]:

$$m_a = 5.3\times 10^{-19}\text{eV}\left(\frac{10^{16}\text{GeV}}{f_a}\right)^4 \tag{2}$$

There are two sources of cold light axions: vacuum misalignment and string decay and domain-wall decay [11]. In the first case, inflation occurs after the PQ phase transition. The axion field is homogenized over enormous distances, and the vacuum misalignment yields axions with the zero-momentum mode and zero velocity dispersion. In the second scenario, the axion field will have random values in different causally connected universe volumes when the PQ phase transition occurs after inflation. This results in the appearance of a network of cosmic strings. The strings disappear after the QCD phase transition, radiating massive axions with momentum of order the Hubble expansion rate. The cold LAs, produced by string decay, have a wide distribution of momentums in their vacuum state and an extremely small velocity dispersion of their excitations [18,27,34]. Primordial axion stars formed by axions with mass $m_a \sim 10^{-6}$ eV, also known as axion clumps, are formed in the early universe shortly after the Big Bang when axions condensed into a dense, gravitationally bound Bose-Einstein condensate. These clumps can range in size and mass, potentially forming compact objects with significant gravitational influence [19–23,29,31].

 doi:10.20944/preprints202408.0033.v1

In modern understanding of galaxy formation, every galaxy forms within a dark matter halo. The formation of galaxy halos is a critical aspect of galaxy formation, providing the gravitational scaffold around which baryonic matter (ordinary matter) accumulates to form stars and galaxies. Primordial axion stars, formed in the early universe, could act as seeds for the formation of larger structures, leading to the formation of galaxies surrounded by halos. Their gravitational influence would attract surrounding dark matter and baryonic matter, facilitating the growth of density perturbations that eventually lead to galaxy formation.

In this paper, we study the formation of the DM stars by ULAs and the relationship between primordial axion stars and galaxy halos. We show that ULA stars, with a size and mass comparable with observable data for typical galaxies of our universe, are formed in the radiation-dominated era.

The paper is organized as follows. Section 1 discusses the cosmological production of axions and the formation of axion stars. In Section 2, we introduce a non-relativistic model describing axion Bose-Einstein condensate. Section 3 summarizes the results obtained and discusses possible generalizations of our approach. Throughout the paper, we use the natural unit convention, $\hbar = c = 1$.

1. Cosmological Production of Axions

We assume the universe is described by ΛCDM model [35,36]. In this model, the universe comprises photons, neutrinos, ordinary (baryon) matter, cold dark matter, and dark energy. The latter is defined by the cosmological constant, Λ, and is responsible for the observable acceleration in the expansion of our universe. The axion DM can be described by a model with the action given by [11,37,38],

$$S = \int \sqrt{-g}\, d^4x \left(\frac{1}{2} g^{\mu\nu} \phi_{,\mu} \phi_{,\nu} - V(\phi) \right). \tag{3}$$

The corresponding equation of motion is the Klein-Gordon equation:

$$\Box\phi = -\frac{\partial V(\phi)}{\partial \phi}. \tag{4}$$

Qualitatively the potential $V(\phi)$, generated by QCD instantons, may be written as [5,11]

$$V(\phi) = (m_a f_a)^2 \left(1 - \cos\left(\phi/f_a\right) \right), \tag{5}$$

where m_a is the axion mass. The potential $V(\phi)$ is the periodic function with a period defined by a shift-invariance, $\phi \to \phi + 2\pi f_a$. There are N degenerate vacua, and the axion field has a range $0 < \phi < 2\pi f_a$ [11].

1.1. Non-Relativistic Limit of the Klein-Gordon Equation

In the non-relativistic limit, the Klein-Gordon equation has the form of the Schrödinger equation with the effective potential describing the interacting forces in the system in the non-relativistic limit [20,21,24,39,40]. Writing,

$$\phi = \frac{1}{2\sqrt{m_a}} \left(\psi e^{-im_a t} + \psi^* e^{im_a t} \right), \tag{6}$$

one can show that the non-relativistic theory is described by the effective action for the complex field ψ (see Appendix **??** for detail):

$$S_{\rm eff} = \int d^4x \Big(\frac{i}{2} (\psi^* \dot\psi - \dot\psi^* \psi) - \frac{1}{2m_a} \nabla\psi^* \cdot \nabla\psi - V_{\rm eff}(\psi^*\psi) - \frac{1}{8\pi G} \nabla\Phi \cdot \nabla\Phi - m_a \psi^* \psi \Phi \Big), \tag{7}$$

Preprints.org (www.preprints.org) | NOT PEER-REVIEWED | Posted: 2 August 2024 doi:10.20944/preprints202408.0033.v1

where $\Phi(\mathbf{r})$ is the Newtonian gravitational potential, and $V_{eff}(|\psi|)$ is the effective potential obtained as the non-relativistic limit of the instanton potential Eq. (5). The equations of motion are given by

$$i\frac{\partial\psi}{\partial t} = -\frac{1}{2m}\nabla^2\psi + m_a\Phi\psi + \frac{\partial V_{\text{eff}}}{\partial\psi^*}\psi,$$
$$\nabla^2\Phi = 4\pi G m_a|\psi|^2. \tag{8}$$

For the axion field, the effective instanton non-relativistic potential potential was derived in Refs. [39,41] and takes the form

$$V_{\text{eff}}\left(\psi^*\psi\right) = \frac{1}{2}m_a\psi^*\psi + m_a^2 f_a^2\left[1 - J_0\left(n^{1/2}\right)\right], \tag{9}$$

where $J_0(z)$ is a Bessel function, $n = \psi^*\psi/n_0$ and $n_0 = m_a f_a^2/2$.

Figure 1 represents the normalized effective potential, $V_0(x) = 1 - J_0(x)$, with the first term subtracted:

$$V_0 = \frac{1}{2mn_0}\left(\mathcal{V}_{\text{eff}} - \frac{1}{2}m_a\psi^*\psi\right) \tag{10}$$

The stable solutions for the axion stars with $n \gg 1$ (dense stars) correspond to the minima of the effective potential [20].

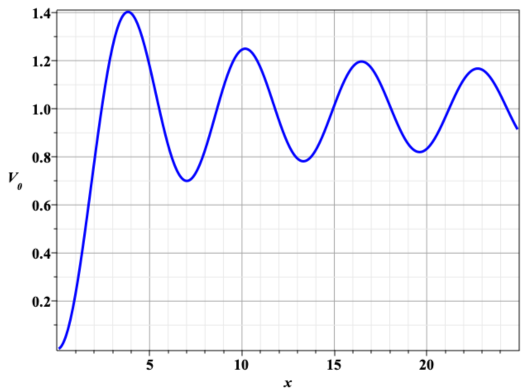

Figure 1. Effective potential: $V_0 = 1 - J_0(x)$.

1.2. Formation of Axion Stars

Axion stars are characterized by their high density and stability, maintained by a balance between gravitational attraction and quantum pressure due to the axions' wave-like nature. They can be categorized into two types:

- **Dilute Axion Stars** ($n_{core} \ll 1$). These stars are less dense and more extended, and insert "their size is determined by "their size is determined by the axion mass and self-interaction strength.
- **Dense Axion Stars** ($n_{core} \gtrsim 1$). These are more compact and can undergo complex dynamical processes, including potential collapse into black holes and phase transition to the dilute stars under certain conditions.

The stability and structure of axion stars are determined by the balance between gravitational attraction and the quantum pressure arising from the Heisenberg uncertainty principle.

2. Model

The non-relativistic axions can form a Bose-Einstein condensate (BEC). The equations that describe a static BEC of axions can be obtained by considering an axion field $\psi(\boldsymbol{r}, t)$ whose time dependence is

$\psi(\boldsymbol{r})\exp(-i\mu t)$, where μ is the chemical potential [20]. They can be expressed conveniently as coupled equations for $\psi(\boldsymbol{r})$ and the gravitational potential $\Phi(\boldsymbol{r})$:

$$\begin{aligned}\nabla^2\hat{\psi} =& 2m_a^2\left(\Phi - \frac{\mu}{m_a} - \frac{1}{2} + \frac{J_1(|\hat{\psi}|)}{|\hat{\psi}|}\right)\hat{\psi},\\ \nabla^2\Phi =& 4\pi G m_a n_0|\hat{\psi}|^2,\end{aligned} \tag{11}$$

where $\hat{\psi} = \psi/\sqrt{n_0}$, $G = 1/m_p^2$, and m_p denotes the Planck mass ($m_p = 1.2\cdot 10^{19}$ GeV). To further simplify matters, we rescale coordinates and functions: $\boldsymbol{r} \to \boldsymbol{r}^* = \boldsymbol{r}/r_0$, $\psi \to \psi(\boldsymbol{r}^*)$ and $\Phi \to \gamma\Phi(\boldsymbol{r}^*)$, where $r_0 = \gamma/m_a$ and $\gamma = m_p/f_a$.

Hereafter, we drop $*$'s in rescaled functions and parameters. Then, the dimensionless equations can be recast as follows:

$$\begin{aligned}\nabla^2\hat{\psi} =& 2\left(\Phi - \gamma\varepsilon\right)\hat{\psi},\\ \nabla^2\Phi =& 4\pi|\hat{\psi}|^2,\end{aligned} \tag{12}$$

where

$$\varepsilon = \bar{\mu} + \frac{1}{2} - \frac{J_1(|\hat{\psi}|)}{|\hat{\psi}|}, \tag{13}$$

and we set $\bar{\mu} = \mu/m_a$.

In Table 1, we present various length and mass scales to facilitate recalculation in physical units. In particular, the mass of the axion star can be obtained using the formula:

$$M = 3M_0\int|\hat{\psi}|^2 d^3V^*, \tag{14}$$

where the integration is performed over dimensionless variables $\mathbf{r}^*$, and $M_0 = 4\pi n_0 r_0^3/3$.

Table 1. Acronyms: f_a - Coupling constant; $M_\odot$ - sun mass; n_{DM} - dark matter density.

Axion mass [eV]	f_a [GeV]	r_0 [pc]	M_0 [$M_\odot$]	n_0 [$1/cm^3$]	$n^* = n_{DM}/n_0$
$5.3\cdot 10^{-23}$	10^{17}	12	$3.59\cdot 10^{14}$	$3.45\cdot 10^{43}$	$7.11\cdot 10^{-19}$
$5.3\cdot 10^{-19}$	10^{16}	$1.2\cdot 10^{-3}$	$3.59\cdot 10^{8}$	$3.45\cdot 10^{45}$	$7.11\cdot 10^{-23}$
$5.7\cdot 10^{-6}$	10^{12}	$1.12\cdot 10^{-18}$	$3.34\cdot 10^{-19}$	$3.71\cdot 10^{46}$	$6.15\cdot 10^{-39}$

Our model is based on the previous studies of the rotating axion stars made in [20,22,23,40,42]. In general ψ may consist of a superposition of various spherical harmonics Y_l^m,

$$\hat{\psi}(r,\theta,\varphi) = \sum_{\ell=0}^{\infty}\sum_{m=-l}^{\ell} f_\ell^m r^\ell Y_\ell^m(\theta,\varphi). \tag{15}$$

For simplicity, we assume the following ansatz:

$$\hat{\psi}(r,\theta,\phi) = R(r)Y_l^m(\theta,\varphi). \tag{16}$$

After substitution of $\hat{\psi}(r,\theta,\phi)$, one can rewrite Eq. (12) as

$$\begin{aligned}&\Delta_r R - \frac{l(l+1)}{r^2}R = 2\left(\Phi - \gamma\bar{\mu} - \frac{\gamma}{2} + \frac{\gamma J_1(R|Y_l^m|)}{R|Y_l^m|}\right)R,\\ &\nabla^2\Phi = 4\pi R^2|Y_l^m|^2,\end{aligned} \tag{17}$$

 doi:10.20944/preprints202408.0033.v1

where Δ_r denotes the radial part of the Laplacian,

$$\Delta_r = \frac{1}{r^2}\frac{\partial}{\partial r}\left(r^2\frac{\partial}{\partial r}\right). \tag{18}$$

Note that (17) still depends on angular variables θ and φ. Therefore, following [40], we take the angular average of these equations. We define the angular averaged gravitational potential and use the normalization of the spherical harmonics:

$$\tilde{\Phi} = \frac{1}{4\pi}\int \Phi(r,\theta,\varphi)d\Omega, \quad \int Y_\ell^m Y_{\ell'}^{m'*} d\Omega = \delta_{\ell\ell'}\delta_{mm'}., \tag{19}$$

$$\mathcal{J}_l^m = \frac{1}{4\pi}\int \frac{J_1(R|Y_l^m|)}{R|Y_l^m|}d\Omega. \tag{20}$$

Then, we obtain for angular averaged potentials the following equations of motion:

$$\Delta_r R = 2\left(\tilde{\Phi} + \frac{l(l+1)}{2r^2} - \gamma\bar{\mu} - \frac{\gamma}{2} + \gamma\mathcal{J}_l^m)\right)R, \tag{21}$$

$$\Delta_r\tilde{\Phi} = R^2. \tag{22}$$

For $l = 0, 1$, we have obtained the analytical expressions for $\mathcal{J}_l^m$. The computation yields:

$$\mathcal{J}_1^0 = J_0(a_0R) - \frac{J_1(a_0R)}{a_0R} + \frac{\pi}{2}\Big(J_1(a_0R)H_0(a_0R) - J_0(a_0R)H_1(a_0R)\Big), \tag{23}$$

$$\mathcal{J}_1^{\pm1} = \frac{1-\cos(a_1R)}{a_1^2R^2}, \quad \mathcal{J}_0^0 = \frac{J_1(R)}{R}, \tag{24}$$

where $a_0 = \sqrt{3/4\pi}$, $a_1 = \sqrt{3/8\pi}$ and $H_n(z)$ denotes the Struve function.

For a given function $R(r)$, the gravitational potential can be obtained due to the integration of Eq. (22). The solution can be written as follows:

$$\tilde{\Phi}(r) = -\frac{1}{r}\int_0^r x^2R^2(x)dx - \int_r^{r_h} xR^2(x)dx, \tag{25}$$

where r_h is the radius of the star. From here it follows that $\tilde{\Phi}(0) = \tilde{\Phi}_0$ and $\Phi'(0) = 0$, where

$$\tilde{\Phi}_0 = -\int_0^{r_h} xR^2(x)dx. \tag{26}$$

We impose the following boundary conditions to solve numerically the coupling system of the differential equations (21) - (22):

$$R(0) = R_0, \quad R(0)' = R_1, \quad \tilde{\Phi}(0) = \Phi_0, \quad \tilde{\Phi}'(0) = 0. \tag{27}$$

The radius of the axion star is obtained as the solution of the equation:

$$\tilde{\Phi}(r_h) = -\frac{M^*(r_h)}{r_h}, \tag{28}$$

where $M^*(r_h) = \int_0^{r_h} x^2R^2(x)dx$ is the scaled mass of the star, $M^* = M/M_0$, and

$$\tilde{\Phi}(r_h) = -\frac{1}{r_h}\int_0^{r_h} x^2R^2(x)dx. \tag{29}$$

Preprints.org (www.preprints.org) | NOT PEER-REVIEWED | Posted: 2 August 2024 doi:10.20944/preprints202408.0033.v1

The chemical potential is subject to the boundary conditions:

$$\bar{\mu} = \left[\frac{1}{\gamma}\left(\tilde{\Phi} + \frac{l(l+1)}{2r^2}\right) + \mathcal{J}_l^m - \frac{1}{2}\right]\Bigg|_{r=r_h} = 0 \tag{30}$$

3. Results and Discussion

Following the procedure outlined in Sect. 2 we have solved numerically the equations of motion (19) - (20) for the axion mass, $m_a = 5.3 \cdot 10^-19$ eV, and the boundary conditions presented below.

- **Dense stars:**

$$R(0) = 6, \quad R(0)' = 0, \quad \Phi(0) = -1.5, \quad \Phi'(0) = 0, (l = 0,\ m = 0).$$

- **Dilute stars:**

$$\begin{aligned} &R(0) = 0.1, \quad R(0)' = 0, \quad \Phi(0) = -0.065, \quad \Phi'(0) = 0, (l = 0,\ m = 0),\\ &R(0) = 0, \quad R(0)' = 10, \quad \Phi(0) = -0.001, \quad \Phi'(0) = 0, (l = 1,\ m = 0),\\ &R(0) = 0, \quad R(0)' = 0.12, \quad \Phi(0) = -0.5, \quad \Phi'(0) = 0, (l = 1,\ m = \pm 1). \end{aligned}$$

The results are summarized in Figure 2 and Table 2. To obtain the redshift, we use the relation $z = n_h/n_{DM}$, where $n_{DM} = \bar{\rho}_{\rm DM}/m_a$ is the average density of DM obtained from the data presented in Refs. [43**?**]: $\bar{\rho}_{\rm DM} = 1.3 \times 10^{-6}{\rm GeV/cm^3}$. As follows from Table 2, the formation of the axion stars begins in the radiation-dominated era, which, according to the ΛCDM model, corresponds to redshift $z \approx (5.244 \cdot 10^3 - 1.47 \cdot 10^{11})$.

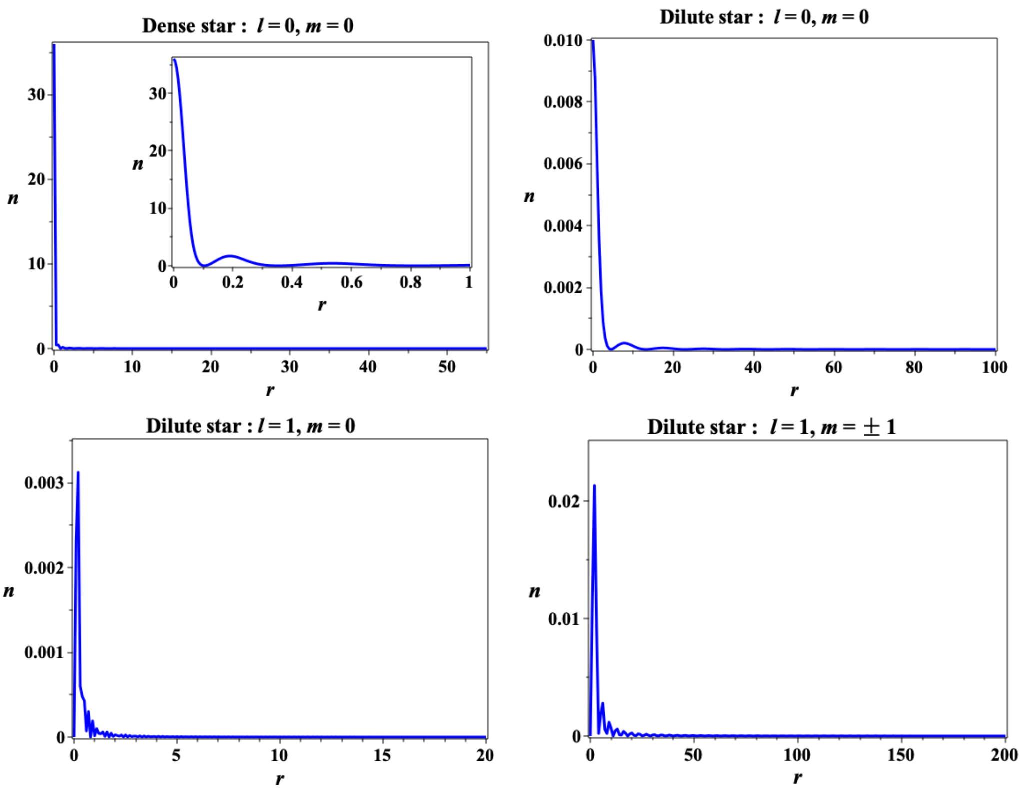

Figure 2. Axion field density, n, vs. dimensionless radial variable r ($m_a = 5.3 \cdot 10^{-19}$ eV). Inset: zoom of the main graph.

Preprints.org (www.preprints.org) | NOT PEER-REVIEWED | Posted: 2 August 2024 doi:10.20944/preprints202408.0033.v1

Table 2. Results of numerical computation.

Angular momentum	Axion mass $m_a = 5.3 \cdot 10^{-19}$ eV			
	Star radius, r_h	Star mass	Density, n_h	Redshift, z
$l = 0, m = 0$	55 [0.06 pc]	43.8 [$1.57 \cdot 10^{10}\ M_\odot$]	$5.86 \cdot 10^{-6}$	$4.35 \cdot 10^5$
$l = 0, m = 0$	350 [0.48 pc]	9.56 [$3.43 \cdot 10^9\ M_\odot$]	$3.58 \cdot 10^{-8}$	$7.96 \cdot 10^4$
$l = 1, m = 0$	410 [0.49 pc]	0.11 [$4 \cdot 10^7\ M_\odot$]	$1.21 \cdot 10^{-12}$	2572
$l = 1, m = \pm 1$	550 [0.66 pc]	109.5 [$3.92 \cdot 10^{10}\ M_\odot$]	$1.77 \cdot 10^{-11}$	6291

The mass of galaxies can vary significantly depending on their type and size:

- Dwarf Galaxies: $M \approx (10^7 - 10^9)M_\odot$.
- Spiral Galaxies: $M \approx (10^{10} - 10^{12})M_\odot$.
- Elliptical Galaxies: $M \approx (10^{12} - 10^{13})M_\odot$.

Considering the distribution of different types of galaxies, the average mass of galaxies in our universe can be roughly estimated as follows: $M \approx 10^{11} M_\odot$. As one can see, the mass of axion stars presented in Table 2 is inside the range of the observable data.

The current size of the axion stars can obtained using the relation: $d = 2zr_h$. We obtain

- $d = 52.2$ kpc ($M = 1.57 \cdot 10^{10}\ M_\odot$)
- $d = 76.4$ kpc ($M = 3.43 \cdot 10^9\ M_\odot$)
- $d = 2.52$ kpc ($M = 4 \cdot 10^7\ M_\odot$)
- $d = 8.3$ kpc ($M = 3.92 \cdot 10^{10}\ M_\odot$)

These results are in agreement with an estimation of the halo size for typical galaxies:

- Spiral Galaxies: 61.3 to 92 kpc in diameter
- Elliptical Galaxies: 92 to 306.6 kpc in diameter
- Dwarf Galaxies: up to 9.2 kpc in diameter

Primordial ULA stars offer potential insights into the nature of dark matter and its role in galaxy formation. As axion stars accrete additional axions, they contribute to the overall density of dark matter halos. This increased density can enhance the gravitational potential of the halo, making it more effective at attracting and retaining baryonic matter. By acting as seeds for structure formation, primordial axion stars could play a pivotal role in the formation of galaxies and shape the universe as we observe it today. Further research is needed to understand their properties, but their potential impact on our understanding of the universe is profound.

Funding: This research received no external funding.

Data Availability Statement: No new data were created or analyzed in this study.

References

1. Kawasaki, M.; Nakayama, K. Axions: Theory and Cosmological Role. *Annual Review of Nuclear and Particle Science* **2013**, *63*, 69–95.
2. Feng, J.L. Dark Matter Candidates from Particle Physics and Methods of Detection. *Annual Review of Astronomy and Astrophysics* **2010**, *48*, 495–545.
3. Bertone, G.; Hooper, D. History of dark matter. *Rev. Mod. Phys.* **2018**, *90*, 045002. https://doi.org/10.1103/RevModPhys.90.045002.
4. Peccei, R.; Quinn, H. CP Conservation in the Presence of Pseudoparticles. *Phys. Rev. Lett.* **1977**, *38*, 1440–1443.
5. Peccei, R.D.; Quinn, H.R. Constraints imposed by CP conservation in the presence of pseudoparticles. *Phys. Rev. D* **1977**, *16*, 1791–1797. https://doi.org/10.1103/PhysRevD.16.1791.
6. Weinberg, S. A New Light Boson? *Phys. Rev. Lett.* **1978**, *40*, 223–226. https://doi.org/10.1103/PhysRevLett.40.223.
7. Wilczek, F. Problem of Strong P and T Invariance in the Presence of Instantons. *Phys. Rev. Lett.* **1978**, *40*, 279–282. https://doi.org/10.1103/PhysRevLett.40.279.

8. Rosenberg, L.J. Dark-matter QCD-axion searches. *Proceedings of the National Academy of Sciences* **2015**, *112*, 12278–12281. https://doi.org/10.1073/pnas.1308788112.
9. Arvanitaki, A.; Huang, J.; Van Tilburg, K. Searching for dilaton dark matter with atomic clocks. *Phys. Rev. D* **2015**, *91*, 015015. https://doi.org/10.1103/PhysRevD.91.015015.
10. Arvanitaki, A.; Dimopoulos, S.; Van Tilburg, K. Sound of Dark Matter: Searching for Light Scalars with Resonant-Mass Detectors. *Phys. Rev. Lett.* **2016**, *116*, 031102. https://doi.org/10.1103/PhysRevLett.116.031102.
11. Sikivie, P., Axion Cosmology. In *Axions: Theory, Cosmology, and Experimental Searches*; Kuster, M.; Raffelt, G.; Beltrán, B., Eds.; Springer Berlin Heidelberg: Berlin, Heidelberg, 2008; pp. 19–50.
12. Chang, S.; Hagmann, C.; Sikivie, P. Studies of the motion and decay of axion walls bounded by strings. *Phys. Rev. D* **1998**, *59*, 023505.
13. di Cortona, G.G.; Hardy, E.; Vega, J.P.; Villadoro, G. The QCD axion, precisely. *Journal of High Energy Physics* **2016**, *2016*, 34. https://doi.org/10.1007/JHEP01(2016)034.
14. Kim, J.E.; Carosi, G. Axions and the strong *CP* problem. *Rev. Mod. Phys.* **2010**, *82*, 557–601. https://doi.org/10.1103/RevModPhys.82.557.
15. Borsanyi, S.; Fodor, Z.; Guenther, J.; Kampert, K.H.; Katz, S.D.; Kawanai, T.; Kovacs, T.G.; Mages, S.W.; Pasztor, A.; Pittler, F.; et al. Calculation of the axion mass based on high-temperature lattice quantum chromodynamics. *Nature* **2016**, *539*, 69–71.
16. Marsh, D.J.E. Axion cosmology. *Physics Report* **2016**, *643*, 1–79, [arXiv:astro-ph.CO/1510.07633]. https://doi.org/10.1016/j.physrep.2016.06.005.
17. Kim, J.E.; Marsh, D.J.E. An ultralight pseudoscalar boson. *Phys. Rev. D* **2016**, *93*, 025027. https://doi.org/10.1103/PhysRevD.93.025027.
18. Yamaguchi, M.; Kawasaki, M.; Yokoyama, J. Evolution of Axionic Strings and Spectrum of Axions Radiated from Them. *Phys. Rev. Lett.* **1999**, *82*, 4578–4581.
19. Jetzer, P. Boson stars. *Physics Reports* **1992**, *220*, 163 – 227. https://doi.org/https://doi.org/10.1016/0370-1573(92)90123-H.
20. Braaten, E.; Mohapatra, A.; Zhang, H. Dense Axion Stars. *Phys. Rev. Lett.* **2016**, *117*, 121801. https://doi.org/10.1103/PhysRevLett.117.121801.
21. Braaten, E.; Zhang, H. Colloquium: The physics of axion stars. *Rev. Mod. Phys.* **2019**, *91*, 041002. https://doi.org/10.1103/RevModPhys.91.041002.
22. Schiappacasse, E.D.; Hertzberg, M.P. Analysis of dark matter axion clumps with spherical symmetry. *Journal of Cosmology and Astroparticle Physics* **2018**, *2018*, 037–037. https://doi.org/10.1088/1475-7516/2018/01/037.
23. Visinelli, L.; Baum, S.; Redondo, J.; Freese, K.; Wilczek, F. Dilute and dense axion stars. *Physics Letters B* **2017**, *777*. https://doi.org/10.1016/j.physletb.2017.12.010.
24. Eby, J.; Mukaida, K.; Takimoto, M.; Wijewardhana, L.C.R.; Yamada, M. Classical nonrelativistic effective field theory and the role of gravitational interactions. *Phys. Rev. D* **2019**, *99*, 123503. https://doi.org/10.1103/PhysRevD.99.123503.
25. Chavanis, P.H. Phase transitions between dilute and dense axion stars. *Phys. Rev. D* **2018**, *98*, 023009. https://doi.org/10.1103/PhysRevD.98.023009.
26. O'Hare, C.A.J. Cosmology of axion dark matter. *PoS* **2024**, *COSMICWISPers*, 040, [arXiv:hep-ph/2403.17697]. https://doi.org/10.22323/1.454.0040.
27. Diez-Tejedor, A.; Marsh, D.J. Cosmological production of ultralight dark matter axions. *arXiv preprint arXiv:1702.02116* **2017**.
28. Du, X.; Behrens, C.; Niemeyer, J.C.; Schwabe, B. Core-halo mass relation of ultralight axion dark matter from merger history. *Phys. Rev. D* **2017**, *95*, 043519. https://doi.org/10.1103/PhysRevD.95.043519.
29. Eby, J.; Leembruggen, M.; Street, L.; Suranyi, P.; Wijewardhana, L.C.R. Global view of QCD axion stars. *Phys. Rev. D* **2019**, *100*, 063002. https://doi.org/10.1103/PhysRevD.100.063002.
30. Eby, J.; Leembruggen, M.; Street, L.; Suranyi, P.; Wijewardhana, L.C.R. Approximation methods in the study of boson stars. *Phys. Rev. D* **2018**, *98*, 123013. https://doi.org/10.1103/PhysRevD.98.123013.
31. Bautista, B.; Degollado, J.C. Static axion stars revisited. *Frontiers in Astronomy and Space Sciences* **2024**, *11*. https://doi.org/10.3389/fspas.2024.1346820.
32. Musoke, N.; Hotchkiss, S.; Easther, R. Lighting the Dark: Evolution of the Postinflationary Universe. *Phys. Rev. Lett.* **2020**, *124*, 061301. https://doi.org/10.1103/PhysRevLett.124.061301.

33. Wechsler, R.H.; Tinker, J.L. The Connection Between Galaxies and Their Dark Matter Halos. *Annual Review of Astronomy and Astrophysics* **2018**, *56*, 435–487. https://doi.org/https://doi.org/10.1146/annurev-astro-081817-051756.
34. Lee, Jae-Weon. Brief History of Ultra-light Scalar Dark Matter Models. *EPJ Web Conf.* **2018**, *168*, 06005. https://doi.org/10.1051/epjconf/201816806005.
35. Frieman, J.A.; Turner, M.S.; Huterer, D. Dark Energy and the Accelerating Universe. *Annual Review of Astronomy and Astrophysics* **2008**, *46*, 385–432.
36. Ryden, B. *Introduction to Cosmology*; Cambridge University Press: New York, NY, USA, 2017.
37. Marsh, D.J. Axion cosmology. *Physics Reports* **2016**, *643*, 1 – 79.
38. Hui, L.; Ostriker, J.P.; Tremaine, S.; Witten, E. Ultralight scalars as cosmological dark matter. *Phys. Rev. D* **2017**, *95*, 043541. https://doi.org/10.1103/PhysRevD.95.043541.
39. Braaten, E.; Mohapatra, A.; Zhang, H. Nonrelativistic Effective Field Theory for Axions. *Phys. Rev.* **2016**, *D94*, 076004, [arXiv:hep-ph/1604.00669]. https://doi.org/10.1103/PhysRevD.94.076004.
40. Davidson, S.; Schwetz, T. Rotating drops of axion dark matter. *Phys. Rev. D* **2016**, *93*, 123509. https://doi.org/10.1103/PhysRevD.93.123509.
41. Eby, J.; Suranyi, P.; Vaz, C.; Wijewardhana, L.C.R. Axion Stars in the Infrared Limit. *JHEP* **2015**, *03*, 080, [arXiv:hep-th/1412.3430]. [Erratum: JHEP11,134(2016)], https://doi.org/10.1007/JHEP11(2016)134,10.1007/JHEP03(2015)080.
42. Miniati, F.; Gregori, G.; Reville, B.; Sarkar, S. Axion-Driven Cosmic Magnetogenesis during the QCD Crossover. *Phys. Rev. Lett.* **2018**, *121*, 021301. https://doi.org/10.1103/PhysRevLett.121.021301.
43. Olive, K. Review of Particle Physics. *Chinese Physics C* **2014**, *38*, 090001. https://doi.org/10.1088/1674-1137/38/9/090001.
44. Planck Collaboration et al. *A &A* **2020**, *641*, A1. https://doi.org/10.1051/0004-6361/201833880.